communications earth & environment

Article

A Nature Portfolio journal

https://doi.org/10.1038/s43247-025-03023-4

Marine darkwave as an event-based framework to assess unusual periods of reduced underwater light availability

François Thoral[1,2] ✉, Matthew H. Pinkerton[2], Shinae Montie[3], Mads S. Thomsen[3,4,5], Christopher N. Battershill[1], Karen Filbee-Dexter[3], Mark Gall[2], Robert J. Miller[6], Shane Orchard[4], Daniel C. Reed[6], Leigh W. Tait[4,7], Spencer D. S. Virgin[4], Thomas Wernberg[3], John Zeldis[8] & David R. Schiel[4]

Episodic reductions in underwater light can be a key driver of marine ecosystem degradation. Yet a consistent event-based framework describing the frequency, duration and intensity of substantial but short-term reductions in underwater light does not exist. Here, we proposed marine darkwaves as a framework for quantifying these episodic reductions of underwater light at specific depths which aligns with definitions of other episodic and extreme events. The framework was applied to long-term in situ time series of underwater irradiance from California, USA (16 years, 6.3 metres) and New Zealand (10 years, at 7 and 20 metres). We showed evidence of several intense marine darkwaves across these sites, with durations up to 64 days, cumulative light deficits reaching −105.6 mol photon·m^{-2}, and up to almost 100% light loss versus climatology. We extended the framework to satellite-derived seabed irradiance data across New Zealand's East Cape region (2002–2023), using a set of 10th percentile threshold and a minimum duration of 5 days. This revealed 25 to 80 spatially varying seabed events, and event durations of 5 to 15 days. Importantly, the framework enables local to continental-scale comparisons of the patterns and ecological consequences of episodic light reduction in marine ecosystems.

A central theme in global change biology is disentangling the consequences of gradual shifts in mean, or "normal" environmental conditions, from those driven by extreme but short-lived events[1]. For example, gradual changes in key environmental conditions like sea temperature, water pH, wave exposure, and dissolved oxygen can drive long-term alterations in marine species distributions, physiological performances, and ecosystem structure[2]. However, related acute extreme events, including marine heatwaves (MHWs)[3] and cold-spells (MCSs)[4], episodic acidification[5], storms[6], and hypoxic (low oxygen) pulses[7], have been shown to cause rapid, and often nonlinear, ecological responses. Extreme short-term events have revealed sudden mass mortalities, population collapses, and ecosystem reconfigurations - impacts that can exceed effects from mean state changes but are also at risk of not being detected in trend analysis of long time series data[8–10]. The interplay and synergies between long-term chronic ("press") and short-term acute ("pulse") disturbances are an active and growing area of research[11]. Despite the sophistication of frameworks developed to detect, characterise and predict the extreme environmental events that affect marine life – as successfully done for temperature anomalies, ocean acidification, deoxygenation, and increased storminess – there remains a conspicuous gap in our understanding of changes to extreme underwater light climates. In this paper, we propose an analogous framework for quantifying episodic reductions in underwater light that we term marine darkwaves (MDWs).

Light availability is, like temperature, pH, oxygen, and wave action, an essential determinant of marine ecosystem structure and functioning. Light intensity and its spectral quality directly control photosynthesis, thereby significantly affecting the diversity and productivity of primary producers, their associated biogeochemical fluxes[12–14] and influencing the distribution and community composition of photoautotrophs[15–17]. Underwater

[1]School of Science, University of Waikato, Tauranga, New Zealand. [2]Earth Sciences New Zealand, Greta Point, Wellington, New Zealand. [3]UWA Oceans Institute and School of Biological Sciences, University of Western Australia, Crawley, WA, Australia. [4]Marine Ecology Research Group, University of Canterbury, Christchurch, New Zealand. [5]Department of Ecoscience, Aarhus University, Roskilde, Denmark. [6]Marine Science Institute, University of California Santa Barbara, Santa Barbara, CA, USA. [7]Earth Sciences New Zealand, Christchurch, New Zealand. [8]Earth Sciences New Zealand, Hamilton, New Zealand.
✉e-mail: francoisthoral@gmail.com

irradiance also alters the behaviour, reproduction and survival of animals and their interactions, especially for visual predators that rely on underwater sighting for catching prey[14]. Long-term changes in climate (e.g., increased precipitation) and human activities (e.g., changed land use practices) have resulted in increased sedimentation and eutrophication that reduce water clarity in near-shore habitats. This gradual degradative process was described by Aksnes et al.[18] as coastal darkening, the biological implications of which are now considered one of the most pressing concerns for coastal ecosystems[19]. For example, coastal darkening and compromised light availability have reduced the productivity and resilience of temperate macroalgal forests[20–22], tropical coral reefs[23], seagrass meadows[24], and microphytobenthic assemblages[25]. Coastal darkening may also exaggerate temperature-driven species range shifts and changes in phenology and behaviour of many coastal marine species[19].

Coastal darkening to date has primarily been concerned with the gradual, long-term decline in water clarity, without strict quantitative criteria for assessing the duration and magnitude of darkening, and an inability to detect short-term variability within long-term trends[18,26]. Importantly, the coastal darkening concept does not quantitatively address the issue of reduced light intensities beyond changes in water clarity, as it has traditionally been measured using Secchi discs and proxies of light absorption[18,26]. In this paper, we shift the focus to the episodic nature of coastal darkening events, for which there is a significant conceptual and analytical framework gap that impedes understanding of how discrete and unusual low-light events affect oceanic and coastal marine ecosystems. Such a framework is necessary for quantitative analysis and comparison between different types of low-light drivers in space and time, which will further motivate researchers to study their biological impacts.

Episodic and abrupt underwater light reduction events have significant ecological effects across a wide range of marine taxa alongside long-term and more diffuse changes (i.e., coastal darkening). A review of 89 coral reef species showed that species-specific survival was both sensitive to the intensity and duration of high turbidity events[27]. Similarly, laboratory experiments demonstrated that just a few days of darkness or low light with intermittent exposure to ambient light impaired physiology and primary productivity of macroalgae[28] and seagrass[29,30], while a mesocosm experiment simulating a 35-day intense darkening decreased phytoplankton biomass and altered community composition[31]. A meta-analysis on marine photoautotrophs spanning 240 experiments from 180 studies further revealed the overall negative and interactive effects of light reduction intensity and duration[32]. Collectively, these studies suggest that short but intense periods of light deprivation can be as detrimental to marine autotrophs as longer and less intense light reduction periods. Less is known about the effects of episodic darkening events on marine heterotrophs relying on vision and photoreception, although a review in elasmobranchs[33] suggests disruption in swimming rhythmicity and behaviour during short-term underwater darkness events. Despite the growing recognition of the ecological effects of short-term (day-to-month) and unusually low underwater irradiance, it is still unclear how frequently such events occur in the coastal and offshore ocean.

In this study, we propose a formal definition for MDWs. We conducted a sensitivity analysis using long-term in situ light time series data from the literature to refine our detection criteria based on empirical variability. We applied this definition to four long-term time series: (1) in situ underwater light dataset from California, USA (at 6.3 metres, case study 1) and (2, 3) in situ (7 and 20 metres, case study 2) and (4) satellite remotely sensed data (on the seabed, case study 3) from New Zealand. We determined the effectiveness of different thresholds for MDW intensity and duration in detecting relatively rare and intense low-light events. Further, we quantified and compared the MDW metrics of the most intense events detected in the four independent case studies. Finally, we discuss some limitations and suggest avenues for future refinement and utility of the MDW framework. Our goal for developing this framework is to facilitate standardised comparisons of episodic low-light events with the aim that they lead to improved monitoring and new insights into the climatic and anthropogenic stressors that cause them and lead to ecological impacts on marine communities.

Results

Sensitivity analysis

Across the three in situ time series, a stricter set of conditions for MDW detection, defined by lower percentile thresholds and higher minimum durations, consistently resulted in a smaller percentage of MDW day occurrences compared to more permissive conditions (Fig. 1A–C, Table 1). For example, applying a 5th percentile threshold with a minimum duration of 5 days yielded MDW day percentages of 1.27%, 0.20%, and 1.68% for the SBC LTER, NZ-FoT-7m, and NZ-FoT-20m case studies, respectively. In contrast, a more permissive combination of a 20th percentile threshold and a minimum duration of 2 days resulted in substantially higher MDW day percentages of 21.11%, 15.09%, and 18.54% for the same sites (Fig. 1A–C, Table 1).

In terms of relative intensity, stricter detection criteria led to higher mean percentage light loss during MDW events compared to climatology (Fig. 1D–F, Table 1). Specifically, the 5th percentile and 5-day duration combination produced mean light deficits of −90.50%, −90.08%, and −92.52% for SBC LTER, NZ-FoT-7m, and NZ-FoT-20m, respectively. Conversely, the 20th percentile and 2-day duration combination resulted in lower mean deficits of −78.67%, −57.24%, and −67.02% across the same sites (Fig. 1D–F, Table 1).

This pattern, where stricter criteria detect fewer but more intense MDWs, is also reflected in absolute metrics such as the number of MDW days, events, and event durations (Fig. S1, Supplementary Information) and mean, maximum, and cumulative intensity (Fig. S2, Supplementary Information). For example, under the strict 5th percentile and 5-day condition, the number of events was limited to 10, 1, and 5 for SBC LTER, NZ-FoT-7m, and NZ-FoT-20m, respectively, with mean durations of 6.60, 7.00, and 12.00 days. In contrast, the lower 20th percentile and 2-day condition yielded 193, 128, and 114 events, with shorter mean durations of 5.70, 4.21, and 5.81 days, respectively. No MDW events were detected under particularly stringent detection conditions, such as a percentile threshold of 1 combined with a minimum duration exceeding 5 days for SBC LTER and NZ-FoT-7m or exceeding 12 days for NZ-FoT-20m (Fig. 1, Table 1).

In terms of trends in the in situ time series, there was a small but significant positive trend in irradiance values (0.04 mol photon·m^{-2}·d^{-1} per year, p-value = 0.03, Fig. S3A, Supplementary Information), equivalent to 1.44 % of change per year compared to the 2008–2024 median (2.53 mol photon·m^{-2}·d^{-1}) in the SBC LTER case study. However, such a small linear trend in the time series did not significantly affect the MDW detection, as similar events were found when applied to the detrended time series (Fig. S3B–D, Supplementary Information). For the two NZ-FoT time series, there were no significant trends for both depths (p-value > 0.05, Fig. S4). However, there was a contrasting negative slope at the 7 m depth (−0.09 mol photon·m^{-2}·d^{-1} per year, −1.2 % cent change per year to 10 yr median) and a positive slope at the 20 m depth (0.01 mol photon·m^{-2}·d^{-1} per year, 1.8% percent change per year to 10 yr median).

Short-term versus long-term MDWs

Across the three case studies, a subset of events co-occurred between the 2-day and 5-day minimum duration thresholds, using a common 10th percentile threshold (Fig. 2, Table S1, Supplementary Information). Co-occurrence was defined as having identical start and end dates across both minimum duration thresholds, indicating events that persist long enough to meet both criteria, and that the subsequent metrics of duration, mean, max, and cumulative intensities were identical. Of all events detected under the 2-day threshold, SBC LTER exhibited 17 co-occurring events (out of 126 total 2-day events, 13.49%, Fig. 2A), NZ-FoT-7m showed 6 co-occurring events (out of 64, 9.38%, Fig. 2B), NZ-FoT-20m had 8 co-occurring events (out of 60, 13.33%, Fig. 2C). Of the total events identified under the 2-day threshold, 219 events did not co-occur with any event under the 5-day threshold, across the three time series. Furthermore, 189 of these (86.3%)

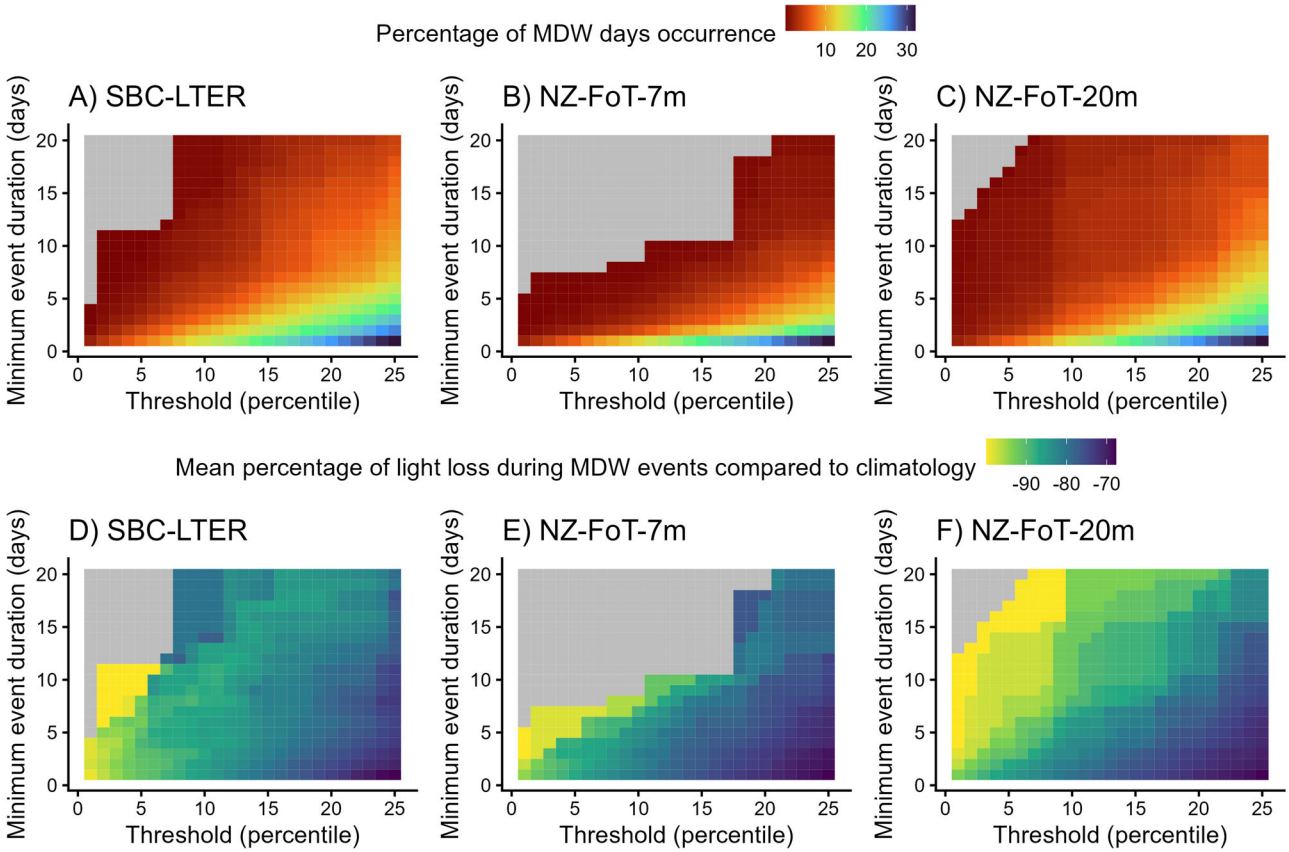

Fig. 1 | Effects of varying minimum durations and threshold percentiles on marine darkwave (MDW) metrics: Percentage of MDW occurrence (top row), and percentage of light loss during MDW events (mean) compared to climatology derived from the full time series (bottom row). The case studies are from Santa Barbara Coastal LTER (**A**, **D**, 6.3 m depth); New Zealand Firth of Thames coastal mooring case study at (**B**, **E**) 7 m and (**C**, **F**) 20 m depths.

were excluded primarily due to their shorter durations (<5 days), which failed to meet the more stringent 5-day criterion. Similarly, out of all events detected under the 5-day threshold, SBC LTER exhibited 9 non-co-occurring events (out of 26 total 5-day events, 34.62%, Fig. 2A), NZ-FoT-7m showed 4 non-co-occurring events (out of 12, 33.33%, Fig. 2B), NZ-FoT-20m had 1 non-co-occurring event (out of 7, 14.29%, Fig. 2C). However, all 14 events were found to partially overlap with a least one 2-day event (Fig. 2, Table S1, Supplementary Information), highlighting some level of complementarity between the two duration criteria.

Vertical synchronicity of MDW events in case study 2

To evaluate the vertical synchronicity of MDW events along the same water column, we analysed temporal overlaps between the NZ-FoT-7m and NZ-FoT-20m time series and under both 2-day and 5-day duration criteria (Fig. 2B, C, Table S1, Supplementary Information). Under the 2-day criterion, 34 total events at 7 m were found to co-occur with events at 20 m depth (58% of all events). These overlaps ranged from brief 2-day events to extended anomalies, such as the 2006–2007 event spanning 23 December to 13 January. However, 25 events at 7 m did not overlap with deeper events, suggesting there were stratification and depth-specific processes. Under the 5-day criterion, only 2 events from NZ-FoT-7m overlapped with 20 m events (29%), indicating that longer-duration anomalies are less frequently synchronised across depths (Fig. S5, Supplementary Information). The remaining 5 events were unique to the 7 m layer, including the intense event from 31 January to 6 February 2006, which did not have a corresponding 20 m counterpart.

Most intense MDWs: case study 1 (SBC LTER)

Under the 5-day minimum duration criterion, the longest and most intense event (in terms of cumulative intensity) began on 10th June 2021, peaked on 6th July, and ended on 9th July, lasting 30 days (Fig. 3A). It reached a mean intensity of −3.82 mol photon·m^{-2}·d^{-1}, a maximum of −3.95 mol photon·m^{-2}·d^{-1}, and a cumulative intensity of −114.67 mol photon·m^{-2}, resulting in a −79.97% light loss related to climatology. This event also appears under the 2-day criterion, confirming its persistence across thresholds. The highest mean (−4.64 mol photon·m^{-2}·d^{-1}) and maximum (−5.13 mol photon·m^{-2}·d^{-1}) intensities were recorded during a 7-day MDW peaking on 15th July 2013, also present in the 2-day dataset. Under the 2-day criterion, the most intense event in terms of both mean (−5.24 mol photon·m^{-2}·d^{-1}) and maximum (−6.18 mol photon·m^{-2}·d^{-1}) intensity occurred during a short MDW from 16th to 17th August 2023, peaking on 17th August (Table S1, Supplementary Information).

Most intense MDWs: case study 2 (NZ-FoT-7m)

The most extreme event under the 5-day criterion occurred from 31st January to 6th February 2006, peaking on 2nd February (Fig. 3B). It lasted 7 days, with a mean intensity of −10.94 mol photon·m^{-2}·d^{-1}, a maximum of −12.61 mol photon·m^{-2}·d^{-1}, and a cumulative intensity of −76.57 mol photon·m^{-2}, equating to a −67.53% light loss related to climatology. This event is also captured under the 2-day criterion. The longest 5-day event lasted 8 days, from 10th to 17th October 2010, with a cumulative intensity of −56.97 mol photon·m^{-2}, equating to a −60.84% light loss related to climatology, and is also present in the 2-day dataset. Under the 2-day criterion, the highest mean intensity (−14.16 mol photon·m^{-2}·d^{-1}) was recorded during a 2-day MDW from 12th to 13th January 2007, peaking on 12th January. The highest maximum intensity (−16.90 mol photon·m^{-2}·d^{-1}) occurred during a separate 2-day event on 8th–9th January 2007, peaking on 9th January (Table S1, Supplementary Information).

Table 1 | Effects of different sets of percentile thresholds and minimum durations on marine darkwave (MDW) detection applied to in situ long-term underwater irradiance time series

Case Study	Threshold (percentile)	Minimum duration	MDW days occurrence (%)	Light loss vs climatology (%)	MDW days	Number of events	Mean duration	Mean intensity	Max intensity	Cumulative intensity mean	Cumulative intensity total
SBC LTER	5	2	4.87	−90.99	254	79	3.22	−3.30	−3.45	−10.60	−837.74
		5	1.27	−90.50	66	10	6.60	−3.33	−3.55	−21.58	−215.80
	10	2	10.67	−85.58	556	126	4.41	−3.08	−3.30	−13.54	−1706.62
		5	4.45	−85.72	232	26	8.92	−3.10	−3.38	−28.37	−737.62
	20	2	21.11	−75.16	1100	193	5.70	−2.78	−3.12	−15.75	−3038.93
		5	12.53	−78.67	653	62	10.53	−2.68	−3.09	−29.16	−1808.03
NZ-FoT-7m	5	2	2.04	−75.53	73	29	2.52	−7.44	−7.92	−18.86	−546.85
		5	0.20	−90.08	7	1	7.00	−7.44	−8.51	−52.05	−52.05
	10	2	5.32	−67.36	190	64	2.97	−6.56	−7.31	−18.34	−1173.59
		5	1.18	−69.34	42	7	6.00	−5.38	−6.61	−33.89	−237.24
	20	2	15.09	−54.44	539	128	4.21	−5.29	−6.62	−21.86	−2798.31
		5	6.69	−57.24	239	29	8.24	−5.53	−7.50	−45.44	−1317.69
NZ-FoT-20m	5	2	3.19	−82.20	114	27	4.22	−0.86	−0.91	−3.66	−98.79
		5	1.68	−92.52	60	5	12.00	−1.25	−1.36	−11.28	−56.41
	10	2	8.65	−74.53	309	60	5.15	−0.82	−0.91	−4.24	−254.13
		5	4.37	−78.89	156	12	13.00	−0.98	−1.13	−11.67	−140.03
	20	2	18.54	−62.81	662	114	5.81	−0.67	−0.79	−4.02	−458.69
		5	10.53	−67.02	376	33	11.39	−0.69	−0.88	−8.56	−282.53

The various metrics shown include the per cent of MDW occurrence, relative mean percentage loss of light during MDW events versus climatology, number of MDW days, events, mean duration of events, mean and max intensity (in mol photon·m^{-2}·d^{-1}), and the mean and total cumulative intensity (in mol photon·m^{-2}) across all MDW events.

Most intense MDWs: case study 2 (NZ-FoT-20m)

The most intense MDW event under the 5-day criterion (in terms of all intensity metrics) occurred from 23rd December 2006 to 13th January 2007, peaking on 9th January (Fig. 3C). It lasted 22 days, with a mean intensity of −2.17 mol photon·m^{-2}·d^{-1}, a maximum of −2.61 mol photon·m^{-2}·d^{-1}, and a cumulative intensity of −47.65 mol photon·m^{-2}, resulting to a −82.15% light loss related to climatology. This event is also present in the 2-day dataset. The longest MDW event lasted 64 days, from 26th July to 27th September 2007, peaking on 27th September, and is also captured under the 2-day criterion. Under the 2-day criterion, the same event from 23rd December 2006 to 13th January 2007 also holds the record for both the highest mean and maximum intensity (Table S1, Supplementary Information).

Case study 3: application of the MDW framework on satellite data (East Cape of New Zealand)

Between 2002 and 2023, there were 25–80 MDWs detected per pixel (0.25 km^2), with a total of 200–800 MDW days per pixel around the East Cape of New Zealand (Fig. 4A, B). On average, events lasted between 5 and 15 days, with a mean maximum intensity of −1 to −25 mol photon·m-^{2}·d-^{1}. Overall, cumulative intensity (i.e., the total deficit of seabed light levels due to MDWs over 21 years) was between −1000 and −5500 mol photon·m^{-2} (Fig. 4C–F). Spatially, MDWs were generally stronger, longer and more frequent at near-shore and shallower portions of the seabed (Fig. 4, Fig. S7, Supplementary Information), although the relationship between MDW metrics and distance to shore displays some variability, especially for the number of MWD days, events, and duration metrics (Fig. S7, Supplementary Information).

Across the East Cape region, pixel-averaged MDW metrics varied between years, where the largest number of MDW days (45) and mean duration of events (~16 days per event), and the lowest mean (−1.5 mol photon·m^{-2}·d^{-1}), maximum (−2.5 mol photon·m^{-2}·d^{-1}), and cumulative (−60 mol photon·m^{-2}) intensities all occurred in 2023 (Fig. 5, largely attributed to Cyclone Gabrielle, see "Methods" and "Discussion" sections). However, the largest number of events occurred in 2004 (4 events). All pixel-averaged MDW metrics did not show significant trends (Fig. 5, Table S2, Supplementary Information). Additionally, all change point years detected were not significant, revealing no change in distribution of the pixel-averaged MDW metrics (Fig. 5, Table S2, Supplementary Information). Collectively, these results do not support either an intensification or reduction in MDW frequency, duration and intensity during the 2002–2023 period. The years 2023 and 2004 were characterised by the most intense MDWs (in terms of strongest cumulative intensity), in the east and west regions, respectively (Fig. 6). Additionally, there were only 2.75 % (396 pixels) and 0.02 % (3 pixels) of pixels with respectively significant positive and negative trends in seabed irradiance across the region (Fig. S8).

Discussion

There is a need for consistent reporting on extreme episodic changes to environmental conditions from daily to monthly time scales, because these types of perturbations, compared to slower and smaller gradual changes, can have more profound and immediate impacts on communities and ecosystem functioning[1,34]. Our proposed MDW framework complements existing approaches for marine heatwaves (MHWs)[3] and cold-spells (MCSs)[4], episodic acidification[5], storm activity[6], and hypoxic (low oxygen) pulses[7], noting that these have successfully been applied at local and global scales to improve understanding of ecological impacts. We leveraged underwater light time series data to test the sensitivity of the proposed MDW framework to various parameters and to demonstrate its utility.

Although the detection of an MDW was sensitive to the choice of percentile threshold and minimum duration period (as all extreme event frameworks are), we showed consistency between MDW metrics across three independent time series, supporting the robustness and general applicability of the framework. For example, some of the most intense MDWs that were identified displayed durations extending up to 64 days, cumulative light deficits reaching −105.6 mol photon·m^{-2}, and light losses

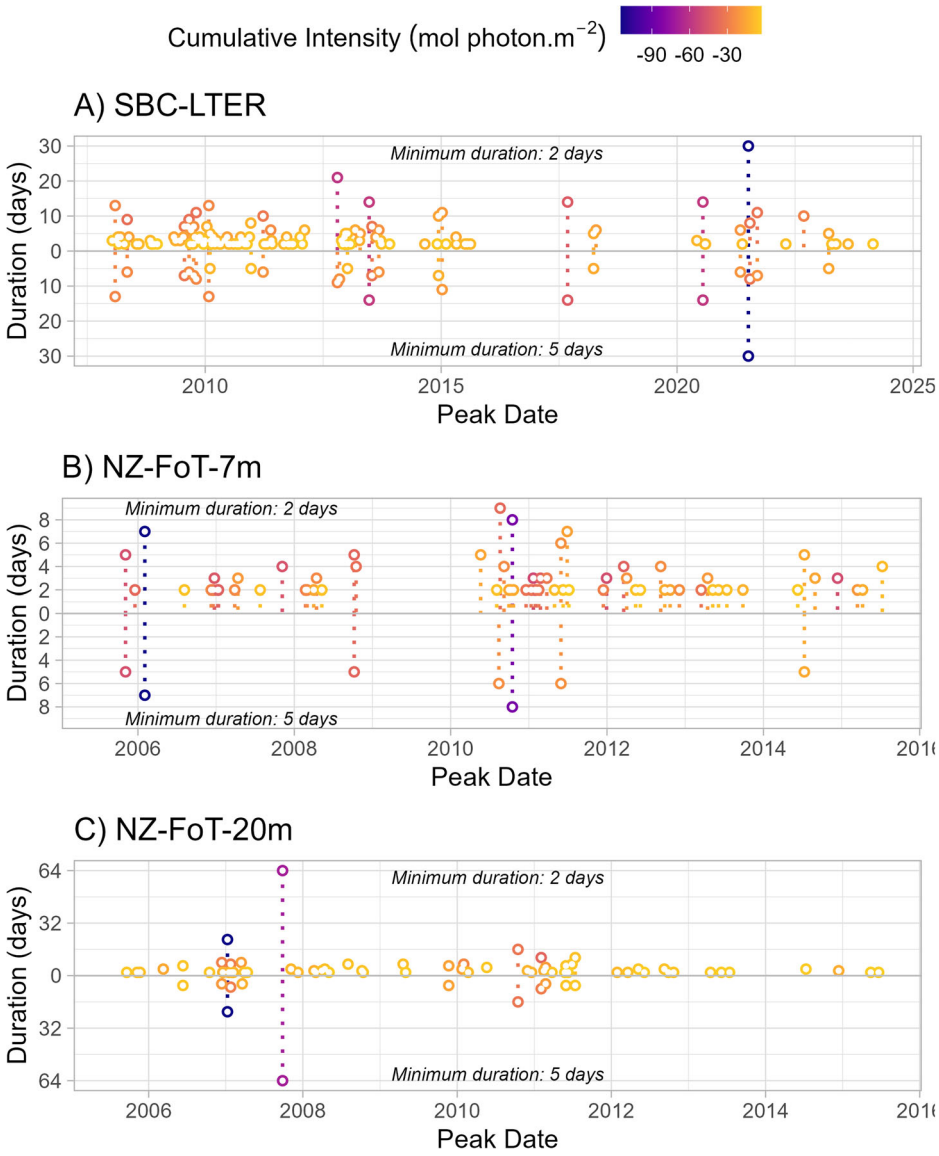

Fig. 2 | Peak date, duration and cumulative intensity of marine darkwaves (MDWs), detected using a relative threshold (10th percentile) and a minimum duration of 2 versus 5 days. The case studies are from Santa Barbara Coastal LTER (**A**, 6.3 m depth); New Zealand Firth of Thames coastal mooring case study at **B** 7 m and **C** 20 m depths.

approaching 100% relative to climatology during peak events. These findings are broadly consistent with observations by Anthony et al.[35] who reported strong 8-week and weaker 2–4-week periodicities in seabed light at a turbid inshore reef on Australia's Great Barrier Reef, following sediment influx from intense rainfall. Their study, however, was limited to a single location and a two-year time series, underscoring the need for further, longer-term, multi-site datasets in capturing the full spectrum of MDW dynamics.

MDWs can be caused by many different drivers (Fig. 7), and our results demonstrate the value of establishing a clear framework to monitor these episodic reductions in underwater light availability from whatever causes. For example, many detected MDWs in Case Study 2 coincided with phytoplankton blooms[36], whereas MDW in Case Study 3 followed extreme rain events and runoff after cyclone Gabrielle[37] in New Zealand. Finally, wildfires, followed by intense rainfall and elevated erosion and runoff, may potentially drive MDW in coastal California (SBC LTER case study 1[38–40]). However, it is likely that different MDW drivers can lead to different ecological effects, through, for example, a different impact on the underwater light spectrum[17], and further improvements on the framework might need to explore driver-specific impacts. Importantly, we also observed differences in depth-specific MDW regimes, likely driven by the stratification of the water column. This result highlights that aquatic event-based oceanic frameworks have both horizontal and vertical characteristics, as increasingly recognised for MHWs[41,42] and of particular importance for extreme anoxia events at depth in stratified waters[43].

As climate change and anthropogenic activities continue to intensify the drivers of underwater light reduction (see Fig. 7), the need for an MDW framework becomes increasingly important. Our analyses suggest that while less strict detection criteria (i.e., a lower threshold and shorter minimal duration) will capture a greater number of events – particularly those of shorter duration – the more intense MDWs were consistently identified across a range of parameter settings. This sensitivity analysis highlights the importance of clearly stating the thresholds and minimal durations used in any given study (with a similar requirement for analysis of other extreme events), especially when assessing compound extreme events, as blending multiple frameworks requires harmonisation of detection criteria. For example, Le Grix et al.[44] showed how important consistent and adaptable detection criteria are when looking at co-occurring MHW and low net primary productivity (MHW-NPPX) events and their ecological impacts.

The MDW framework will help researchers and environmental managers to identify causes and implications of light-driven ecological change by providing comparability between diverse studies across an array of marine systems. A growing number of studies already suggest that episodic and abrupt reductions in underwater light can have significant

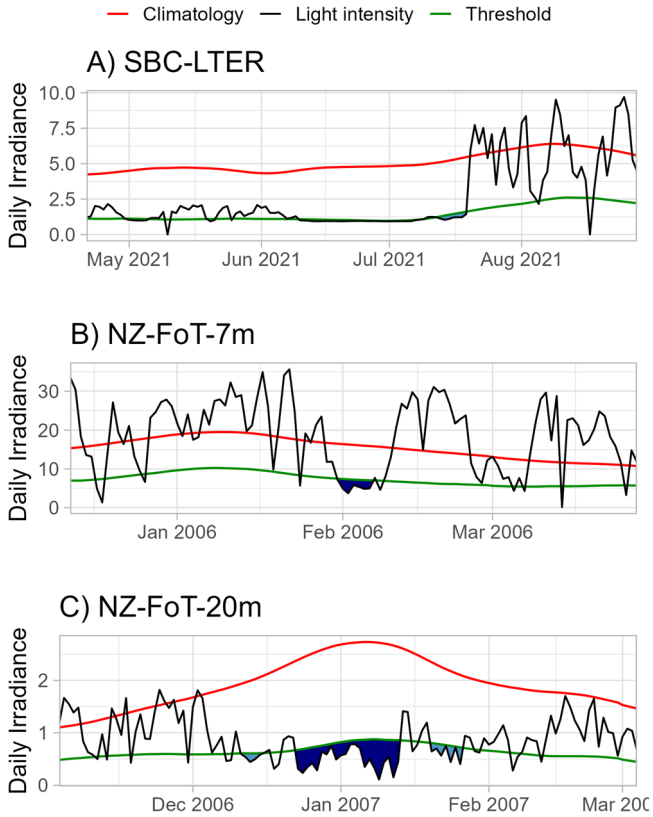

Fig. 3 | Evidence of in situ marine darkwaves. Underwater daily irradiance time series (dark, in mol photon·m^{-2}·d^{-1}), climatology (red) and 10th percentile threshold (green) for the SBC LTER (**A**, 6.3 m), NZ-FoT-7m (**B**), and NZ-FoT-20m (**C**) case studies. The most intense marine darkwaves (MDWs, using a 5-day minimum duration) in terms of cumulative intensity are highlighted in dark blue, while other less intense events are shown in light blue.

biological effects across a wide range of marine taxa[32]. Experimental studies on seagrasses, macroalgae, and phytoplankton have demonstrated that even short-term exposure to low or no light – ranging from a few days to several weeks – can significantly impair photosynthesis, growth, and survival[27–31], however, without reporting on observed low-light events. Our study confirms that such biologically relevant light reduction events from mesocosm experiments are occurring naturally at similar temporal scales. Specifically, we detected MDWs lasting from just a few days (depending on the minimum duration) to >60 days, with cumulative light deficits reaching 100% relative to the climatological conditions, which align or exceed those used in experimental stress scenarios. These findings suggest that future research could be strengthened by integrating analyses of multiple MDW metrics, similar to how the MHW framework has stimulated extensive research by allowing comparison between metrics, regions and taxa[45].

Perhaps the single strongest limitation to analysing MDWs to date relates to the shortage of high-quality long-term in situ light data. Moored underwater sensors that record high frequency of instantaneous light intensity in situ are well suited to capture the variability in light availability across a wide range of temporal scales[35]. However, such high-quality data are scarce globally, poorly resolved spatially, and their duration typically falls below the recommended 30-year period to derive more robust climatological baselines[3]. Furthermore, shorter time series data are susceptible to a shifting baseline syndrome, where the climatological threshold will be skewed towards higher or lower underwater light values[46,47]. By comparison, the longer time series encompasses more climatic variability and can therefore better characterise the normal baseline conditions. We therefore recommend a more systematic global research effort to support existing (and establish new) long-term in situ time series of underwater and seabed light, and, more specifically, developing standardised protocols to calibrate remotely sensed data to stimulate analysis of MDWs. Nonetheless, Schlegel et al.[48] showed that time series shorter than 30 years can produce acceptable MHW metrics, which may suggest this is also the case for MDWs. In this study, we showed that there were little to no effects of relatively small linear trends in the MDW detection. One strength of this framework is to allow for the detection of depth-specific events; however, it cannot be representative of the whole water column, unless applied to an array of sensors deployed along the water column, or vertically-resolved light models[49]. Furthermore, the framework will not be relevant for applying in deep-sea conditions, where there is no light. Additionally, adapting the framework to finer temporal resolution (sub-daily or tidally aware event detection) might prove useful in shallow ecosystems, where tidal variability dominates, particularly for organisms or communities responding on shorter timescales of light delivery. Finally, we have demonstrated application on the PAR (400–700 nm) range, but future studies could apply the framework on spectral intensity time series, and further identify coloured MDWs, i.e., reduction of particular wavelengths at depths of interest.

Recently, satellite remote sensing of seabed light has emerged as a promising approach to enhance our spatial understanding of low-light events, massively extending the capability of the limited in situ, point-based measurements (analogous to the rise in MHW analysis from satellite-based temperature products). Individual sensor deployments provide poor spatial resolution, need to be regularly checked and cleaned, and consequently, the costs are very high. However, satellite products of benthic light availability in the shallow coastal zone have now been generated at regional[50–53] and even global scales[13,54], leveraging up to 25 years of ocean colour remote sensing time series. We believe these products can provide unprecedented yet untapped opportunities to study MDWs and their possible ecological impacts. Specifically, we showed that MDWs, as a coherent framework to assess unusual events of reduced underwater light intensity, could be applied to both in situ and remotely sensed time series, similar to other extreme event detection frameworks, such as MHWs[3], or low net primary production extremes[44].

Although satellite remote sensing of seabed light holds great promise, many challenges remain. For example, satellite time series are frequently missing data, in the same way that in situ instruments can suffer from sensor malfunction, loss of power, limits on data storage capacity and instrument loss. Limited satellite data arises from limited image acquisition (not taking images at the right time and place), faulty sensors[55], high cloud cover, failure in atmospheric correction[56], near-infra-red "glow" due to land and cloud adjacency[57], sea roughness, sun glint, seabed reflectance[58], pixel geo-localisation errors, and/or failure of in-water algorithms[59,60]. For example, it remains a key challenge to estimate MDWs following episodic cyclones, typhoons or hurricanes and extreme precipitation and runoff events, because these events co-occur with a high cloud cover (and therefore no clear ocean images). MDW detection will also be sensitive to 'gap-filling techniques' (interpolation methods used to fill data gaps), as seen for MHW detection[48]. Future work should therefore investigate the effects of gap-filling algorithms on MDW properties, notably by leveraging suitable, long-term in situ underwater light data. Nevertheless, global satellite-based products of underwater light and subsequent MDW metrics will undoubtedly improve dramatically in the near future and become more easily accessible, for example, by following the example of the marine heatwaves tracker[61].

We hope the MDW framework will motivate researchers to explore drivers and attributes of episodic low-light events and stimulate research into their biological impacts. We look forward to leveraging the MDW framework to deepen our understanding of effects across anthropogenic stressors, habitats, ecosystems, geographical regions and time-periods – by combining experimental, in situ, and modelling practices with state-of-the-art remote sensing analysis, and by adopting integrated land-to-sea approaches, that link river catchment processes to the receiving marine environment[62–64].

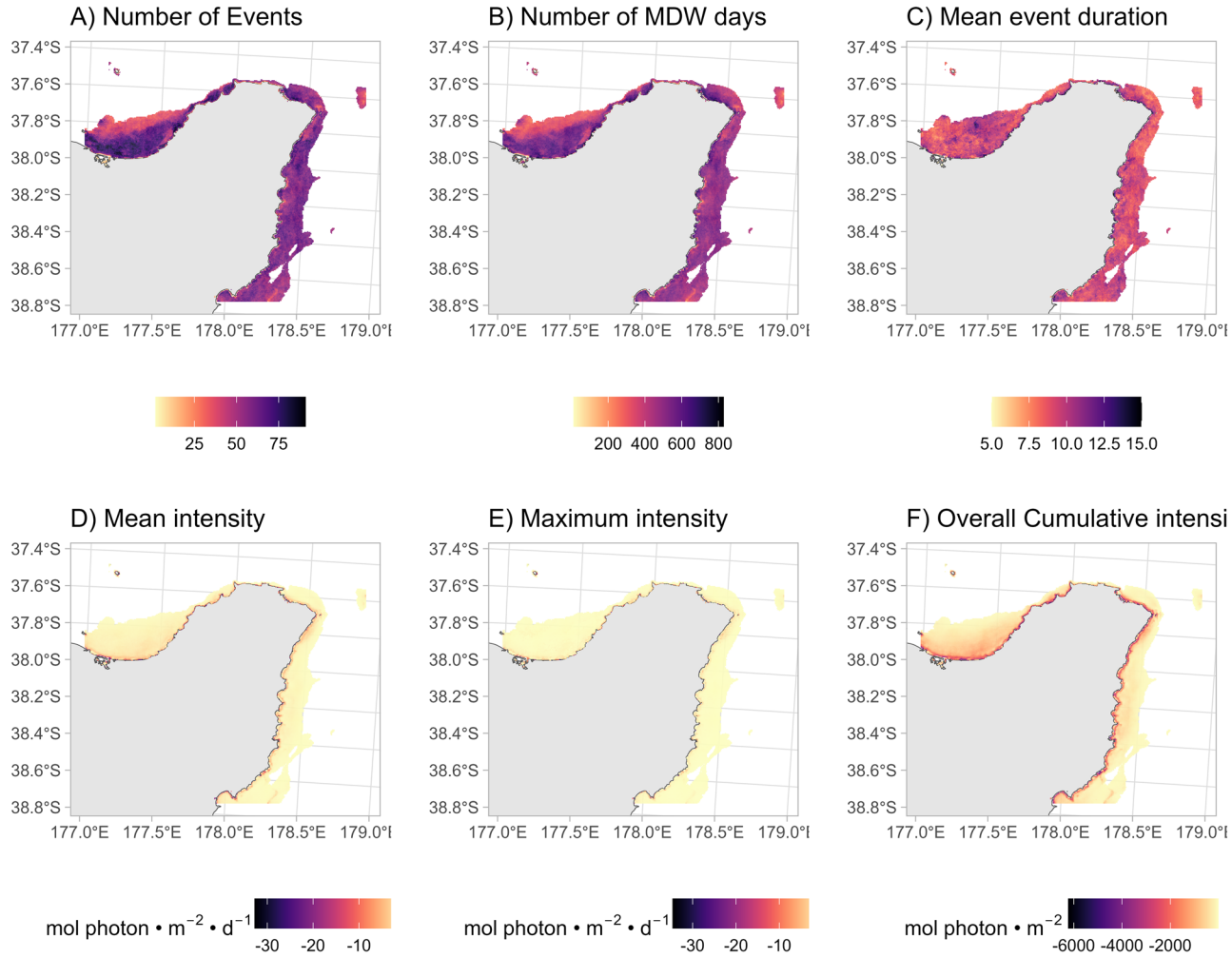

Fig. 4 | Marine darkwave (MDW) metrics per pixel averaged or summed across the 07/2002 to 08/2023 period around the East Cape of New Zealand using satellite data calculated at the seabed. Metrics include **A** Number of total events, **B** Number of total MDW days, **C** Mean event duration, **D** Mean intensity of events, **E** Maximum intensity of events, and **F** Overall cumulative intensity. Only pixels with seabed light levels above 0.01 mol photon·m^{-2}·d^{-1} (using the 21-year median) are shown.

Methods

Defining the marine darkwave framework

General principles. Quantifying extreme darkening events requires clearly-defined metrics that encapsulate the intensity and duration of underwater light across timescales that match the variability of the underlying drivers[7]. We used the following guidelines proposed by Gruber et al.[7] to reduce the arbitrariness[65] of how parameters for extreme event metrics were selected, outlining key choices (*italics*):

(1) *Should the threshold be a relative or absolute value?* A relative threshold (e.g., a 90th percentile) is based on local variability and typically used where affected organisms are adapted to ambient conditions and stressed by deviations. A relative threshold is commonly applied to better assess biological impacts at the ecosystem level, and is used in the standard definition of MHWs[3] and MCSs[4]. By comparison, absolute thresholds (e.g., a specific temperature, water oxygen concentration or pH value) may instead be applied to study the response of a specific species or population with well-defined physiological limits, as done, for example, in the definition of hypoxia[43] and high acidity[66] events;

(2) *Should the baseline be fixed or shifting?* For relative thresholds, the baseline is the period over which the probability function is constructed and from which the thresholds (i.e., the 90th percentile) are derived. In the case of the MHW definition, a fixed baseline of (usually) 30 years, between 1982 and 2011, is often applied, although a shifting baseline approach has also been adopted, using a more recent time interval[67];

(3) *Should thresholds be derived from seasonally varying data (to reflect biological relevance like life-stage dependency[68]) or from de-seasonalised data?* Both approaches have been used to analyse marine extreme events, but their influence on data analysis and interpretations remains an open research question[7];

(4) *What should the minimum duration be to identify an event?* The chosen minimum duration (e.g., 5 days is typically used to define an MHW, whereas shorter events are referred to as 'spikes'[3]) should help to distinguish extreme events from common short-term fluctuations. The chosen duration should also help to identify events with possible biological implications, and not simply reflect statistical noise.

Underwater light availability changes across a wide range of temporal scales driven by both natural and anthropogenic processes (Fig. 7)[59]. While diurnal cycles, seasonal shifts, and long-term climatic trends all contribute to variability, we focused on drivers that operate from days to months because these time scales are likely to be more relevant for identifying and analysing episodic low-light events and linking them to the biological impacts. These events can be climate-driven through sustained cloudiness[69], associated with heavy rain and elevated riverine input of terrigenous sediments, dissolved and particulate organic matter[70,71] and nutrients, or also caused by

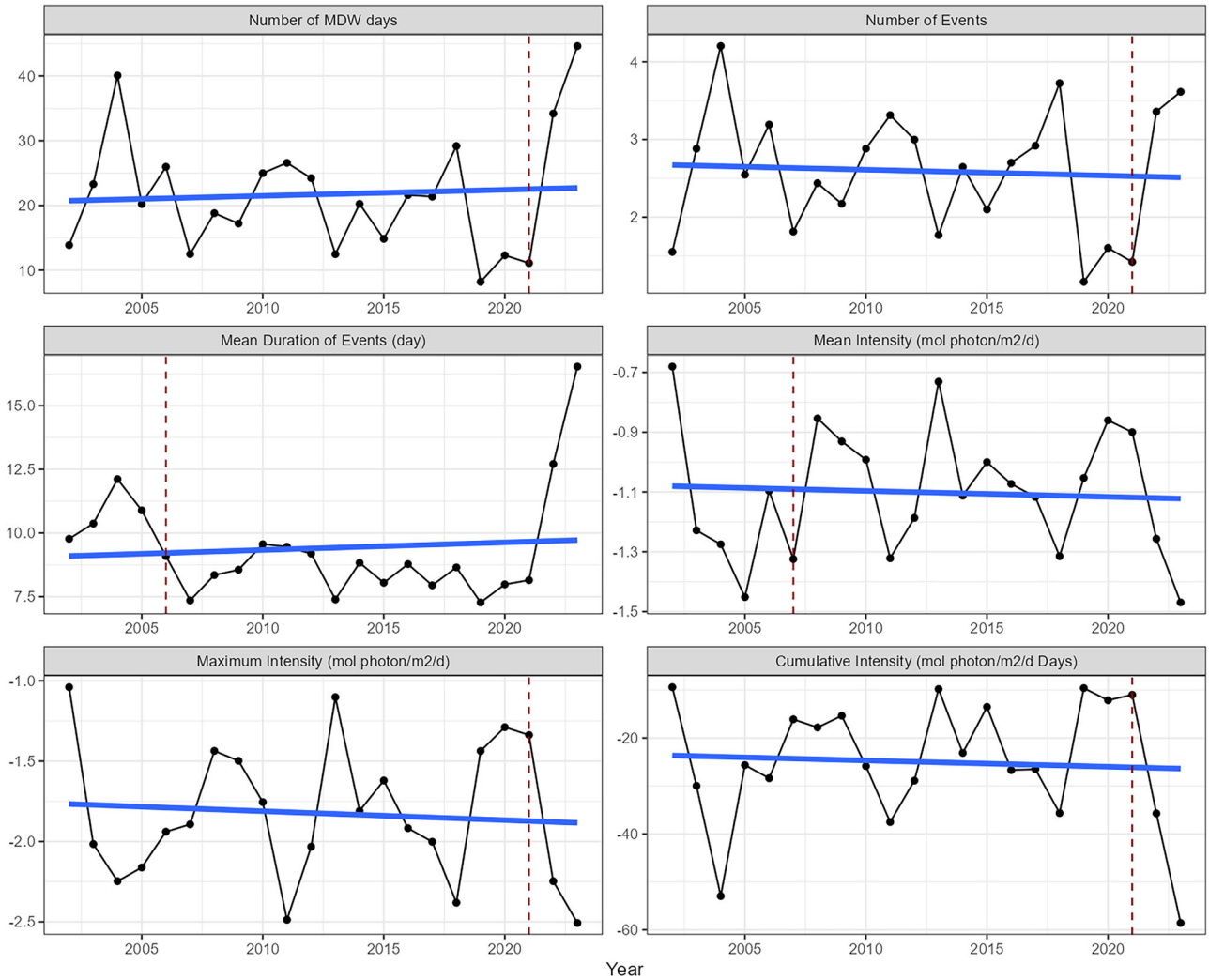

Fig. 5 | Yearly and pixel-averaged MDW metrics for the period 2002–2023 on the seabed around the East Cape of New Zealand using satellite data (in black), as well as linear regression (blue lines) and change point year (red dashed lines, all non-significant *p*-value >0.05). Prior to averaging the metrics per pixel (n = 14,390), the number of MDW days, events and cumulative intensity are summed, whereas the duration, mean, and maximum intensity metrics are averaged per year.

phytoplankton and cyanobacterial bloom[72], and through local resuspensions of marine sediments from wind, waves, and currents (Fig. 7)[35]. Furthermore, episodic reduction in light availability can result from human activities, such as local dredging[73], discharge of municipal and industrial waste[74], altered catchment usage such as agriculture, logging, livestock[75–78] and urbanisation and hard structures[79,80]. Finally, episodic low-light events can be accelerated by climate change through increased precipitation and floods[75], storms and wave resuspension[6], wildfires[39,81], and glacial thawing[82].

MDW definition. Here, we propose a formal definition for MDWs based on daily-integrated irradiance as the primary temporal unit for underwater light availability, thereby minimising the influence of intra-day variability and diurnal cycles (Fig. 8). To identify MDW events, we propose using a relative, seasonally varying, and depth-specific threshold, which accounts for natural fluctuations across season, latitude and depth, based on many years of historical data. This approach ensures that darkness induced by season, latitude and depth does not inherently bias the detection of anomalous events. For example, an MDW should not be solely induced by shorter days in winter in higher latitudes. Similarly, depth should not be an unaccounted source of variation for MDWs when comparing time series between two sites of different depths. For baseline selection, we also recommend a fixed baseline that uses the entire available time series of light data to better assess covarying trends and long-term changes.

MDW parameterisation. All MDWs were detected using the 'heatwaveR' R package (version 0.4.6). This algorithm is the benchmark when it comes to detecting marine thermal extreme events, but it can be widely applied to any daily time series. The algorithm and related metrics are further described in Hobday et al.[3], Schlegel et al.[4], Schlegel and Smit[83], and here we treat MDWs as analogous to marine cold-spells[4]. More specifically, we used a seasonally varying climatology approach to calculate the climatological baseline and threshold percentiles for MDW detection, following the default values implemented in the heatwaveR package. This method applies a sliding window centred on each day of the year to pool values from surrounding days across all years in the time series. Specifically, we use the default 11-day window (5 days before and after, plus the centre day) to calculate the climatological mean and percentile thresholds for each day of the year. This approach accounts for natural seasonal variability in irradiance. To reduce short-term variability and ensure smoother climatological curves, a moving average smoothing is applied to both the climatology and threshold time series. We used the default value of 31 days, which applies a 31-day moving average to the climatological and threshold values, minimising the

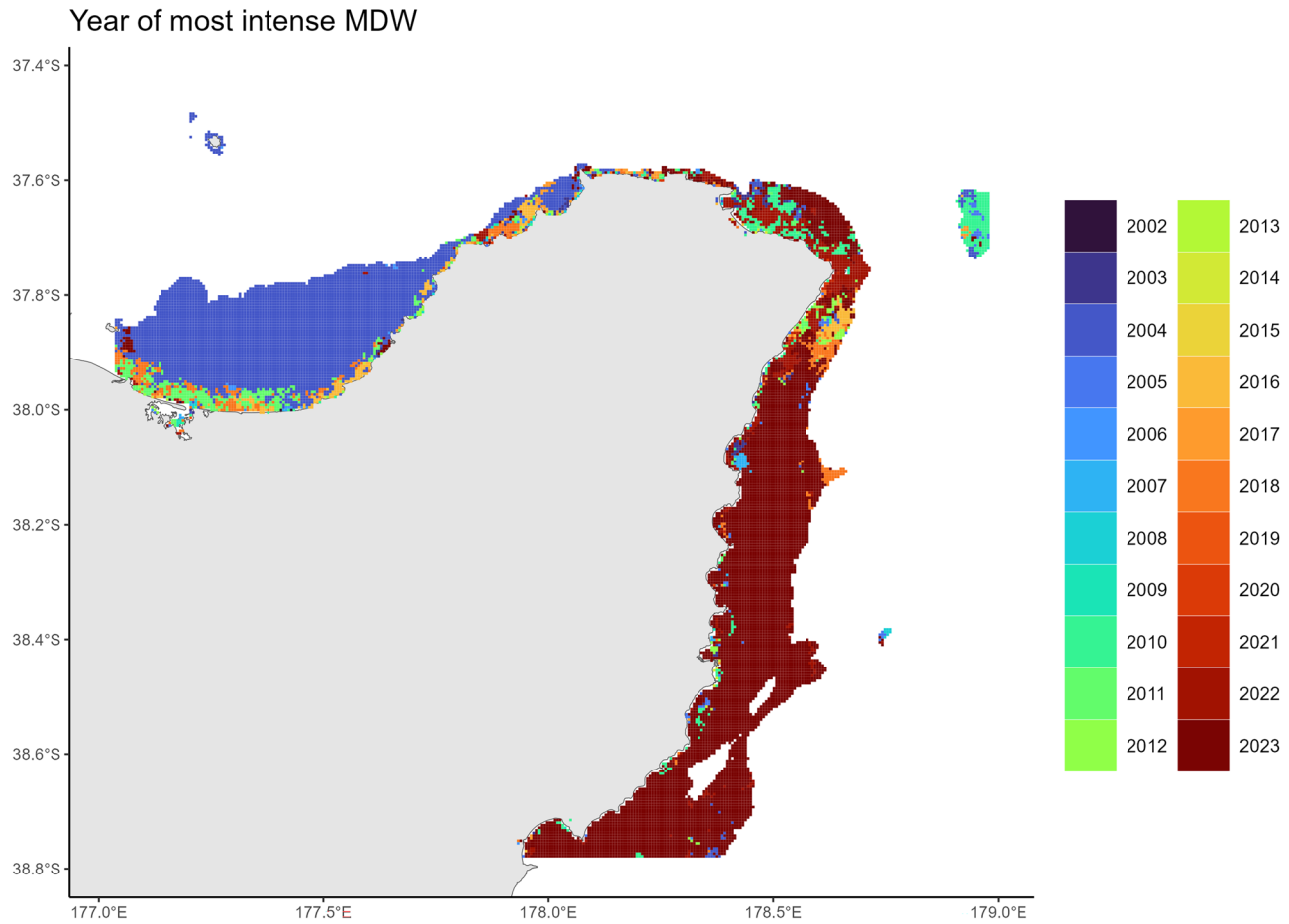

Fig. 6 | Year of the most intense MDW on the seabed in terms of cumulative intensity around the East Cape of New Zealand using satellite data. Only pixels with seabed light levels above 0.01 mol photon·m^{-2}·d^{-1} (using the 21-yr median) are shown.

influence of anomalous single-day values on MDW detection. In the case of minimum durations being set as higher than 2 days, we considered a MDW to be a single event if there are 2 or 1 days between two detected events (as for MHW and MCS), and events shorter than the minimum days criteria were treated as marine dark spikes (MDSs) and are not considered as MDWs following our definition, in alignment with marine heat and cold spikes[3,4]. The choice of length and type of historical baselines (fixed, detrended, shifting, adapting) is crucial when defining MDWs, as it must account for the period over which measurements are taken and the timing of the stressors that reduce underwater light. Different lengths and types of baselines can yield varying interpretations of darkwave characteristics, affecting the assessment of ecosystem risks and management strategies, as shown with MHWs[67]. Therefore, selecting an appropriate baseline for the question of interest ensures accurate representation of the stressor's influence and facilitates effective communication among scientists, policymakers, and the public. In climatology, the usual minimum duration of a reference period is 30 years[84], but the duration of most underwater light time series, including our three case studies, is shorter than this. Here, we chose a fixed baseline that covers the full length of each case study time series and report on potential linear trends within the baseline period of the three case studies.

MDW metrics. For each of three case studies, we calculated and analysed MDW metrics, as defined in Hobday, et al.[3] but applied on underwater irradiance time series, including its duration (difference between end and start, in days), intensity (difference between climatological mean and daily irradiance, a time series in mol photon·m^{-2}·d^{-1}), mean intensity (average of intensity measured each day during a MDW, in mol photon·m^{-2}·d^{-1}), maximum intensity and peak date (amount and day of the highest intensity during a MDW, in mol photon·m^{-2}·d^{-1} and date, respectively), and cumulative intensity (sum of the daily intensities during a MDW, in mol photon·m^{-2}). Importantly, because the MDW concept focuses on less, not more, light compared to the normal light climate, all intensity metrics were reported as negative values.

Case studies

The first two case studies represent in situ measurements from a single geographical location (therefore providing a single set of MDW metrics), whereas the third case study is based on satellite images for which the number of adjacent locations depended on image resolution (i.e., each pixel has its own set of MDW metrics). MDW detection was on the daily-integrated time series of irradiance in a systematic way across all three case studies, regardless of light sensor types, sampling rate and duration.

Case study 1: SBC LTER time series. We used data from the Santa Barbara Coastal Long Term Ecological Research (SBC LTER), which measured underwater light at five locations on shallow subtidal reefs off Santa Barbara, California (USA), from 2008 and is still being maintained[85]. We analysed seabed light data collected at Carpinteria Reef (34° 23.474′N, 119° 32.510′W, named 'CARP 7', at 6.3 metre depth (Mean Lower Low Water), hereafter SBC LTER case study). This site was chosen because it had a long uninterrupted time series (2008-01-12 and 2024-05-10 = 5968 days, i.e., c. 16 years and 4 months) during which it was mostly a sea urchin barren. Because of this, the light sensor had minimal shading from the canopy-forming giant kelp (*Macrocystis pyrifera*) and understory macroalgal species. Importantly, this site is located directly offshore

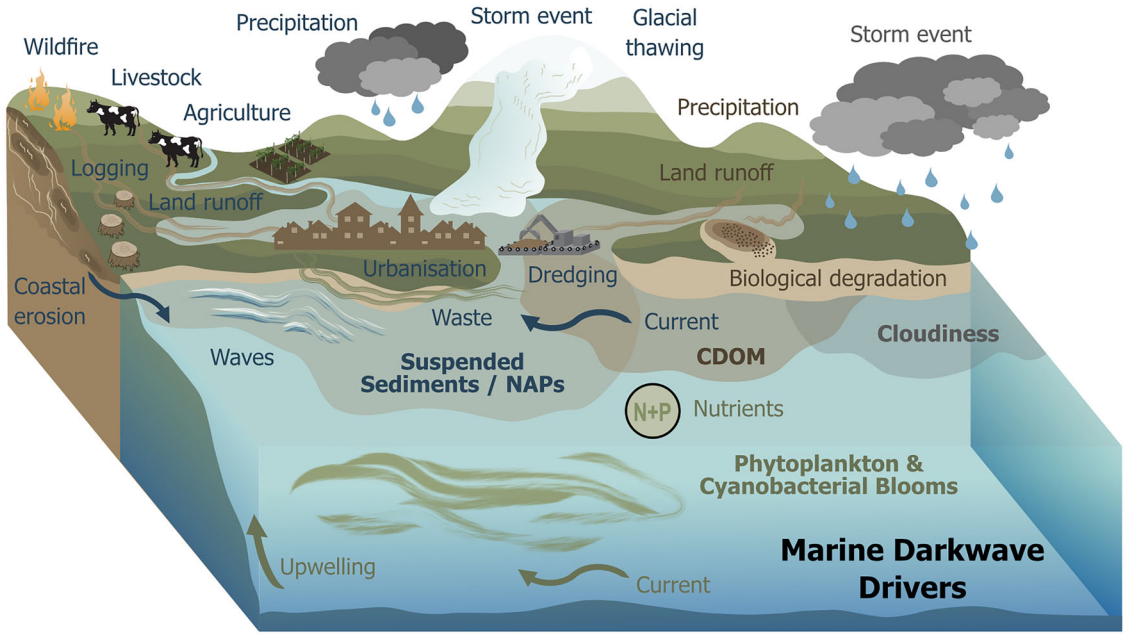

Fig. 7 | Conceptual overview showing primary and secondary drivers of marine darkwaves and underwater light variability at day-to-monthly scales. 'Primary drivers' (bold text) refers to the direct cause of light variability in the water column, affecting light attenuation and sea-surface light. 'Secondary drivers' (normal text) refers to the underlying processes that lead to changes in the primary drivers, for example, precipitation (secondary driver) that increases land runoff of suspended sediment (primary driver). Symbols courtesy of the Integration and Application Network (ian.umces.edu/symbols/, CC BY-SA 4.0), from public domain (CC0), or made by the authors.

of a creek mouth (Santa Monica and Franklin Creeks) that drains an agricultural watershed, and is therefore exposed to episodic riverine sediment and nutrient runoff events that are usually brief but intense during winter storms and minimal or absent between storms[86] as well as variable chlorophyll-*a* (hereafter chl-*a*) concentration values due to phytoplankton blooms[87]. The nearby coastline is also prone to coastal erosion from human developments and natural processes, which can result in additional sediment delivery[40,88].

Irradiance was recorded one to two times per minute from 2008 to 2015 with submersible spherical PAR sensors (MKV-L, Alec Electronics, Japan) and from 2016 to the present with submersible planar PAR sensors (DEFI-L, Alec Electronics, Japan). Conversions from planar to spherical values were applied as described in Reed and Miller[85]. Measurements were averaged over each hour, and data are presented as daily-integrated irradiance in units of mol photon·m^{-2}·d^{-1}. Optical sensors were frequently replaced (i.e., every 6–12 weeks) with newly serviced sensors. The effects of biological fouling were assessed and corrected when needed as described in Reed and Miller[85].

Case study 2: in situ New Zealand Firth of Thames coastal mooring at 7 and 20 m. Our second case study includes two time series from the New Zealand Firth of Thames mooring (36° 45′S, 175° 16′E, hereafter NZ-FoT-7m and NZ-FoT-20m case studies)[36,89]. This site represents typical 'case-1' water conditions (around 95% of the time) where phytoplankton is the main contributor to light attenuation[90]. Exposure to riverine discharges of sediment occurs for only 5% of the time, creating 'case-2 waters', when suspended solids, coloured dissolved organic matter and phytoplankton co-occur to cloud the waters.

Irradiance (μmol photon·m^{-2}·s^{-1}) in the PAR range (400–700 nm) was simultaneously recorded at 7 and 20 m depths, at 10-min intervals using integrating Natural Fluorometers (INF-300, Biospherical Inc. [36]). Bromine was used to prevent biofouling. Instant PAR recordings were integrated daily (to mol photon·m^{-2}·d^{-1}). The time series spans July 2005 to July 2015 (3652 days, ca. 10 years). We also compared MDW metrics between the two depths to look for depth-synchronous events.

Case study 3: Remote sensing of seabed light around the New Zealand East Cape region. A satellite-based time series was used as our third case study. The values for seabed irradiance around the East Cape region of New Zealand were obtained from MODIS-Aqua ocean colour[51,53]. This region is characterised by steep hills in river catchments that are subject to high precipitation rates (1000 to >7000 mm per year on average[91]) and major rainfall and wave events produced by cyclones such as Bola in 1988[92] and Gabrielle in 2023[37]. Additionally, land uses in the region have had widespread changes, from deforestation of indigenous forests between the 1890s and 1920s for conversion to pasture, then to non-native pine planting and harvesting[91,93] which have predisposed the formation of highly erodible gullies[93]. As a result, this region has the highest erosion and sediment yields in New Zealand, with >55 Mt of suspended sediment transported annually into the ocean, which equates to around 0.3% of global suspended sediment[91]. In the coastal zone, this sediment causes periods of intense plumes and turbidity events[94].

Satellite level 1A reflectances (R_{rs}) were atmospherically corrected, converted to inherent optical properties, and used to calculate the diffuse attenuation coefficient of downwelling PAR irradiance[51,95]. Daily level 3 products of K_dPAR were projected onto a New Zealand Transverse Mercator grid (NZTM2000) at a 500 m pixel resolution to match the New Zealand bathymetry grid[96]. MODIS-Aqua sea-surface PAR (E_{0+}PAR) products were obtained daily at 4 km pixel resolution and resampled at 500 m resolution. Daily K_dPAR and sea-surface PAR products were checked for missing values and linearly interpolated in the case of missing values, as recommended in marine heatwave detection[48]. Daily irradiance on the seabed (Ebed, in mol photon·m^{-2}·d^{-1}) was calculated at each pixel location combining light at the sea surface, light attenuation and bathymetry[13,50–52,97]. The time series used spans August 2002 to July 2023 (7669 days, ca. 21 years) for the region bounded by 37° 24′S, 177°E, 38° 45′S 177°E, 38° 45′S, 177°E, 38° 45′S, 179°E. We restricted the analysis to pixels where annual median seabed light was above 0.01 mol photon·m^2·d^{-1} (14,390 pixels, 3597.5 km^2), which included depths between 0.01 to 110 m (Fig. S6, Supplementary Information) and distance to shore between 0.5 and 32 km.

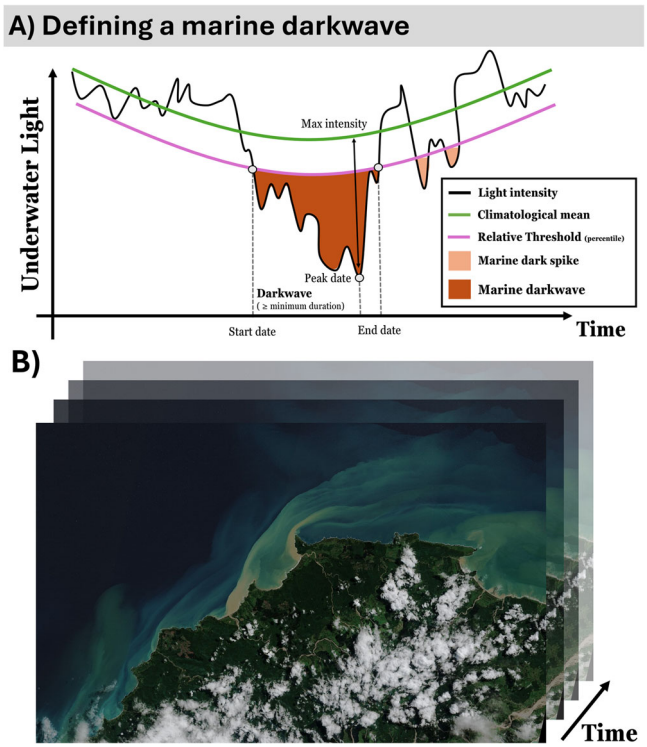

Fig. 8 | Marine darkwave as a conceptual framework. A Conceptual definition of the marine darkwave framework applied to an underwater light time series at a specific depth and location. **B** Sentinel-2 (ESA) image of the East Cape of New Zealand (Whangaparāoa Cape Runaway, −37.54, 177.97) following ex-tropical cyclone Gabrielle on the 14th February 2023, showing the extent of sediment plumes discharging to coastal waters and subsequent potential marine darkwave (modified from Copernicus Sentinel data 2025, accessed via Sentinel Hub EO Browser, https://apps.sentinel-hub.com/eo-browser/. Accessed 4 Mar 2025).

Applying the MDW framework to the case studies

Sensitivity analysis of thresholds and minimum duration

To assess the sensitivity of MDWs detection to set percentile threshold and minimum duration criteria, we detected MDWs under a varying set of percentile thresholds (1st–25th percentile) and minimum duration (2–20 days), such that a range of very strict (low percentile and high minimum duration values) and more permissive (higher percentile, lower minimum duration) conditions were tested. In addition to the previously described absolute metrics of occurrence, duration and intensities, we defined two additional relative metrics that allowed for a robust comparison between the time series, regardless of their length and depth. We defined and calculated the percentage of MDW days occurrence as the ratio between the number of MDW days detected over the total number of days in the time series (in %). We also defined and calculated the percentage of light loss during an MDW event compared to the climatology (in %), which informs the overall loss or deficit in light intensity across events and in relative terms. The sensitivity was carried over the in situ time series, i.e., SBC LTER, NZ-FoT-7m, and NZ-FoT-20m.

Trend analysis

To report on potential trends within the baseline period of the three case studies, we calculated linear trends and their statistical significance in the daily-integrated irradiance time series using the Theil–Sen estimator (Sen's slope hereafter) and modified Mann–Kendall test (R package "modifiedmk" version 1.6), which is more robust in autocorrelated (induced by seasonality) time series. Sen's slope and Mann–Kendall tests have several advantages over classical linear regression for assessing trends in time series, notably a lesser sensitivity to outliers and a distribution-free reliance[98,99]. We reported annual trends (being the slope multiplied by 365), their relative percentage change compared to the long-term median, and trend slope significance (p-value < 0.05).

Mann–Kendall, Sen's slope, and Pettit change point tests were also calculated for annually and pixel-averaged MDW metrics in the New Zealand satellite data case study to assess any changes in MDW activity at the regional scale. Non-parametric Pettitt change point tests were done to detect shifts in central tendency, which would indicate significant changes in the temporal dynamics (change point years, i.e., significant inflexion points in the metric time series), using the R package "trend" (version 1.1.6, Pohlert[99]).

Data availability

In situ time series LTER[85]: https://doi.org/10.6073/pasta/9a42207dd4d2971cce4273fd8a1087b4 (Accessed 2025-03-04). NIWA-SCENZ satellite products[97]: https://gis.niwa.co.nz/portal/apps/experiencebuilder/template/?id=9794f29cd417493894df99d422c30ec2&page=NIWA-SCENZ (Accessed 2025-03-04). R package to detect marine heatwaves and cold-spells[83]: https://robwschlegel.github.io/heatwaveR/ (Accessed 2025-03-04). Post-processed versions of the data used to generate the figures are archived at https://doi.org/10.5281/zenodo.17509746.

Code availability

R script to generate the figures is archived at https://doi.org/10.5281/zenodo.17509746.

Received: 26 March 2025; Accepted: 12 November 2025;
Published online: 12 January 2026

References

1. Jentsch, A., Kreyling, J. & Beierkuhnlein, C. A new generation of climate-change experiments: events, not trends. *Front. Ecol. Environ.* **5**, 365–374 (2007).
2. Poloczanska, E. S. et al. Responses of marine organisms to climate change across oceans. *Front. Mar. Sci.* https://doi.org/10.3389/fmars.2016.00062 (2016).
3. Hobday, A. J. et al. A hierarchical approach to defining marine heatwaves. *Prog. Oceanogr.* **141**, 227–238 (2016).
4. Schlegel, R. W., Darmaraki, S., Benthuysen, J. A., Filbee-Dexter, K. & Oliver, E. C. J. Marine cold-spells. *Prog. Oceanogr.* https://doi.org/10.1016/j.pocean.2021.102684 (2021).
5. Burger, F. A., John, J. G. & Frölicher, T. L. Increase in ocean acidity variability and extremes under increasing atmospheric CO2. *Biogeosciences* **17**, 4633–4662 (2020).
6. Feehan, C. J., Filbee-Dexter, K., Thomsen, M. S., Wernberg, T. & Miles, T. Ecosystem damage by increasing tropical cyclones. *Commun. Earth Environ.* https://doi.org/10.1038/s43247-024-01853-2 (2024).
7. Gruber, N., Boyd, P. W., Frolicher, T. L. & Vogt, M. Biogeochemical extremes and compound events in the ocean. *Nature* **600**, 395–407 (2021).
8. Sampaio, E. et al. Impacts of hypoxic events surpass those of future ocean warming and acidification. *Nat. Ecol. Evol.* **5**, 311–321 (2021).
9. Wernberg, T. et al. An extreme climatic event alters marine ecosystem structure in a global biodiversity hotspot. *Nat. Clim. Chang.* **3**, 78–82 (2012).
10. Smith, K. E. et al. Biological impacts of marine heatwaves. *Ann. Rev. Mar. Sci.* https://doi.org/10.1146/annurev-marine-032122-121437 (2022).
11. Raymond, C. et al. Understanding and managing connected extreme events. *Nat. Clim. Chang.* **10**, 611–621 (2020).
12. Falkowski, P. G., Barber, R. T. & Smetacek, V. Biogeochemical controls and feedbacks on ocean primary production. *Science* **281**, 200–206 (1998).

13. Gattuso, J.-P., Gentili, B., Antoine, D. & Doxaran, D. Global distribution of photosynthetically available radiation on the seafloor. *Earth Syst. Sci. Data* **12**, 1697–1709 (2020).
14. McFarland, W. N. Light in the sea—correlations with behaviors of fishes and invertebrates. *Am. Zool.* **26**, 389–401 (1986).
15. Luimstra, V. M., Verspagen, J. M., Xu, T., Schuurmans, J. M. & Huisman, J. Changes in water color shift competition between phytoplankton species with contrasting light-harvesting strategies. *Ecology* **101**, e02951 (2020).
16. Stomp, M. et al. Adaptive divergence in pigment composition promotes phytoplankton biodiversity. *Nature* **432**, 104–107 (2004).
17. Thoral, F., Pinkerton, M. H., Tait, L. W. & Schiel, D. R. Spectral light quality on the seabed matters for macroalgal community composition at the extremities of light limitation. *Limnol. Oceanogr.* https://doi.org/10.1002/lno.12318 (2023).
18. Aksnes, D. L. et al. Coastal water darkening and implications for mesopelagic regime shifts in Norwegian fjords. *Mar. Ecol. Prog. Ser.* **387**, 39–49 (2009).
19. Herbert-Read, J. E. et al. A global horizon scan of issues impacting marine and coastal biodiversity conservation. *Nat. Ecol. Evol.* **6**, 1262–1270 (2022).
20. Blain, C. O., Hansen, S. C. & Shears, N. T. Coastal darkening substantially limits the contribution of kelp to coastal carbon cycles. *Glob. Chang. Biol.* https://doi.org/10.1111/gcb.15837 (2021).
21. Mangan, S., Tait, L. W., Gerrity, S. & Schiel, D. R. Loss and replacement of macroalgal standing stock and productivity after a major environmental disturbance. *Ecosphere* https://doi.org/10.1002/ecs2.4674 (2023).
22. Tait, L. W., Thoral, F., Pinkerton, M. H., Thomsen, M. S. & Schiel, D. R. Loss of Giant Kelp, Macrocystis pyrifera, Driven by Marine Heatwaves and Exacerbated by Poor Water Clarity in New Zealand. *Frontiers in Marine Science* **8** https://doi.org/10.3389/fmars.2021.721087 (2021).
23. Fabricius, K. E., Logan, M., Weeks, S. & Brodie, J. The effects of river run-off on water clarity across the central Great Barrier Reef. *Mar. Pollut. Bull.* **84**, 191–200 (2014).
24. Ralph, P. J., Durako, M. J., Enríquez, S., Collier, C. J. & Doblin, M. A. Impact of light limitation on seagrasses. *J. Exp. Mar. Biol. Ecol.* **350**, 176–193 (2007).
25. Mangan, S. et al. Shady business: the darkening of estuaries constrains benthic ecosystem function. *Mar. Ecol. Prog. Ser.* **647**, 33–48 (2020).
26. Davies, T. W. & Smyth, T. Darkening of the global ocean. *Glob. Chang. Biol.* **31**, e70227 (2025).
27. Erftemeijer, P. L., Riegl, B., Hoeksema, B. W. & Todd, P. A. Environmental impacts of dredging and other sediment disturbances on corals: a review. *Mar. Pollut. Bull.* **64**, 1737–1765 (2012).
28. Blain, C. O., Rees, T. A. V., Christine Hansen, S. & Shears, N. T. Morphology and photosynthetic response of the kelp Ecklonia radiata across a turbidity gradient. *Limnol. Oceanogr.* **65**, 529–544 (2020).
29. Wong, M. C., Vercaemer, B. M. & Griffiths, G. Response and recovery of Eelgrass (Zostera marina) to chronic and episodic light disturbance. *Estuaries Coasts* **44**, 312–324 (2020).
30. Biber, P. D., Kenworthy, W. J. & Paerl, H. W. Experimental analysis of the response and recovery of Zostera marina (L.) and Halodule wrightii (Ascher.) to repeated light-limitation stress. *J. Exp. Mar. Biol. Ecol.* **369**, 110–117 (2009).
31. Mustaffa, N. I. H. et al. Coastal ocean darkening effects via terrigenous DOM addition on plankton: an indoor mesocosm experiment. *Front. Mar. Sci.* https://doi.org/10.3389/fmars.2020.547829 (2020).
32. Striebel, M. et al. Marine primary producers in a darker future: a meta-analysis of light effects on pelagic and benthic autotrophs. *Oikos* https://doi.org/10.1111/oik.09501 (2023).
33. Carroll, D. & Harvey-Carroll, J. The influence of light on elasmobranch behavior and physiology: a review. *Front. Mar. Sci.* https://doi.org/10.3389/fmars.2023.1225067 (2023).
34. Ummenhofer, C. C. & Meehl, G. A. Extreme weather and climate events with ecological relevance: a review. *Philos. Trans. R. Soc. Lond. B Biol. Sci.* https://doi.org/10.1098/rstb.2016.0135 (2017).
35. Anthony, K. R., Ridd, P. V., Orpin, A. R., Larcombe, P. & Lough, J. Temporal variation of light availability in coastal benthic habitats: effects of clouds, turbidity, and tides. *Limnol. Oceanogr.* **49**, 2201–2211 (2004).
36. Gall, M., Zeldis, J., Safi, K., Wood, S. & Pinkerton, M. Vertical stratification of phytoplankton biomass in a deep estuary site: implications for satellite-based net primary productivity. *Front. Mar. Sci.* https://doi.org/10.3389/fmars.2023.1250322 (2024).
37. Stone, D. A. et al. Cyclone Gabrielle as a design storm for Northeastern Aotearoa New Zealand under anthropogenic warming. *Earths Future* https://doi.org/10.1029/2024ef004772 (2024).
38. Berberian, L. A. et al. Impacts of Wildfire Runoff on Giant Kelp in Malibu, California. In *IGARSS 2024-2024 IEEE International Geoscience and Remote Sensing Symposium*, 5935–5939 (IEEE, 2024).
39. Cira, M. et al. Turbidity and fecal indicator bacteria in recreational marine waters increase following the 2018 Woolsey Fire. *Sci. Rep.* **12**, 2428 (2022).
40. Coombs, J. S. & Melack, J. M. Initial impacts of a wildfire on hydrology and suspended sediment and nutrient export in California chaparral watersheds. *Hydrol. Process.* **27**, 3842–3851 (2012).
41. Zhang, Y., Du, Y., Feng, M. & Hobday, A. J. Vertical structures of marine heatwaves. *Nat. Commun.* **14**, 6483 (2023).
42. Malan, N. et al. Lifting the lid on Marine Heatwaves. *Prog. Oceanogr.* https://doi.org/10.1016/j.pocean.2025.103539 (2025).
43. Codiga, D. L., Stoffel, H. E., Oviatt, C. A. & Schmidt, C. E. Managed nitrogen load decrease reduces chlorophyll and hypoxia in warming temperate urban estuary. *Front. Mar. Sci.* https://doi.org/10.3389/fmars.2022.930347 (2022).
44. Le Grix, N., Zscheischler, J., Rodgers, K. B., Yamaguchi, R. & Frölicher, T. L. Hotspots and drivers of compound marine heatwaves and low net primary production extremes. *Biogeosciences* **19**, 5807–5835 (2022).
45. Benthuysen, J. A., Oliver, E. C., Chen, K. & Wernberg, T. Advances in understanding marine heatwaves and their impacts. *Front. Mar. Sci.* **7**, 147 (2020).
46. Amaya, D. et al. Marine heatwaves need clear definitions so coastal communities can adapt. *Nature* **616**, 29–32 (2023).
47. Sen Gupta, A. & Burrows, M. Marine heatwaves: definition duel heats up. *Nature* **617**, 465–465 (2023).
48. Schlegel, R. W., Oliver, E. C., Hobday, A. J. & Smit, A. J. Detecting marine heatwaves with sub-optimal data. *Front. Mar. Sci.* **6**, 737 (2019).
49. Renosh, P. R., Zhang, J., Sauzède, R. & Claustre, H. Vertically resolved global ocean light models using machine learning. Remote Sens. 15, 5663 (2023).
50. Magno-Canto, M. M., McKinna, L. I. W., Robson, B. J. & Fabricius, K. E. Model for deriving benthic irradiance in the Great Barrier Reef from MODIS satellite imagery. *Opt. Express* **27**, A1350–A1371 (2019).
51. Gall, M. P., Pinkerton, M. H., Steinmetz, T. & Wood, S. Satellite remote sensing of coastal water quality in New Zealand. N. Z. J. Mar. Freshw. Res. 56, 585–616 (2022).
52. Singh, R. K. et al. Satellite-Derived Photosynthetically Available Radiation at the Coastal Arctic Seafloor. *Remote Sens.* https://doi.org/10.3390/rs14205180 (2022).
53. Thoral, F. *Seabed Irradiance in a Warming World*. PhD thesis, Univ. Canterbury (2023).
54. Gattuso, J. P. et al. Light availability in the coastal ocean: impact on the distribution of benthic photosynthetic organisms and their contribution to primary production. *Biogeosciences* **3**, 489–513 (2006).
55. Franz, B. A. et al. The continuity of ocean color measurements from SeaWiFS to MODIS. In *Earth Observing Systems X*. Vol. 5882, 304–316 (SPIE, 2005).

56. Siegel, D. A., Wang, M., Maritorena, S. & Robinson, W. Atmospheric correction of satellite ocean color imagery: the black pixel assumption. *Appl. Opt.* **39**, 3582–3591 (2000).
57. Feng, L. & Hu, C. Land adjacency effects on MODIS Aqua top-of-atmosphere radiance in the shortwave infrared: statistical assessment and correction. *J. Geophys. Res. Oceans* **122**, 4802–4818 (2017).
58. Reichstetter, M. et al. Bottom reflectance in ocean color satellite remote sensing for coral reef environments. *Remote Sens.* **7**, 16756–16777 (2015).
59. Kirk, J. T. *Light and Photosynthesis in Aquatic Ecosystems* (Cambridge Univ. Press, 1994).
60. IOCCG. *Uncertainties in Ocean Colour Remote Sensing* (International Ocean Colour Coordinating Group, Dartmouth, Canada, 2019).
61. https://www.marineheatwaves.org/tracker.html, last accessed 26/09/2025, 2025).
62. Cottrell, R. S. et al. Considering land-sea interactions and trade-offs for food and biodiversity. *Glob. Chang Biol.* **24**, 580–596 (2018).
63. Orchard, S. et al. River Radii: a comparative national framework for remote monitoring of environmental change at river mouths. *Remote Sens.* https://doi.org/10.3390/rs17081369 (2025).
64. Schiel, D. R. & Howard-Williams, C. Controlling inputs from the land to sea: limit-setting, cumulative impacts and ki uta ki tai. *Mar. Freshw. Res.* https://doi.org/10.1071/mf14295 (2016).
65. Stephenson, D. B., Diaz, H. & Murnane, R. Definition, diagnosis, and origin of extreme weather and climate events. *Clim. Extremes Soc.* **340**, 11–23 (2008).
66. Hauri, C., Gruber, N., McDonnell, A. M. P. & Vogt, M. The intensity, duration, and severity of low aragonite saturation state events on the California continental shelf. *Geophys. Res. Lett.* **40**, 3424–3428 (2013).
67. Smith, K. E. et al. Baseline matters: Challenges and implications of different marine heatwave baselines. *Prog. Oceanogr.* https://doi.org/10.1016/j.pocean.2024.103404 (2024).
68. Thoral, F. et al. Unravelling seasonal trends in coastal marine heatwave metrics across global biogeographical realms. *Sci. Rep.* **12**, 7740 (2022).
69. Bélanger, S., Babin, M. & Tremblay, J. É Increasing cloudiness in Arctic damps the increase in phytoplankton primary production due to sea ice receding. *Biogeosciences* **10**, 4087–4101 (2013).
70. Chen, Z., Doering, P. H., Ashton, M. & Orlando, B. A. Mixing behavior of colored dissolved organic matter and its potential ecological implication in the Caloosahatchee River estuary, Florida. *Estuaries Coasts* **38**, 1706–1718 (2014).
71. Yamamoto, K., DeVries, T., Siegel, D. A. & Nelson, N. B. Quantifying biogeochemical controls of open ocean CDOM from a Global Mechanistic Model. *J. Geophys. Res. Oceans* https://doi.org/10.1029/2023jc020691 (2024).
72. Wroblewski, J. S. A model of the spring bloom in the North Atlantic and its impact on ocean optics. *Limnol. Oceanogr.* **34**, 1563–1571 (2003).
73. Fraser, M. W. et al. Effects of dredging on critical ecological processes for marine invertebrates, seagrasses and macroalgae, and the potential for management with environmental windows using Western Australia as a case study. *Ecol. Indic.* **78**, 229–242 (2017).
74. Foster, M. S. & Schiel, D. R. Loss of predators and the collapse of southern California kelp forests (?): alternatives, explanations and generalizations. *J. Exp. Mar. Biol. Ecol.* **393**, 59–70 (2010).
75. Fabricius, K. E., De'ath, G., Humphrey, C., Zagorskis, I. & Schaffelke, B. Intra-annual variation in turbidity in response to terrestrial runoff on near-shore coral reefs of the Great Barrier Reef. *Estuar., Coast. Shelf Sci.* **116**, 57–65 (2013).
76. Hale, R. et al. Hindcasting estuary ecological states using sediment cores, modelled historic nutrient loads, and a Bayesian network. *Front. Mar. Sci.* https://doi.org/10.3389/fmars.2024.1374869 (2024).
77. Klein, R. D., Lewis, J. & Buffleben, M. S. Logging and turbidity in the coastal watersheds of northern California. *Geomorphology* **139-140**, 136–144 (2012).
78. Waterhouse, J., Brodie, J., Lewis, S. & Mitchell, A. Quantifying the sources of pollutants in the Great Barrier Reef catchments and the relative risk to reef ecosystems. *Mar. Pollut. Bull.* **65**, 394–406 (2012).
79. Dudley, B. D., R. Burge, O., Plew, D. & Zeldis, J. Effects of agricultural and urban land cover on New Zealand's estuarine water quality. *N. Z. J. Mar. Freshw. Res.* **54**, 372–392 (2020).
80. Seers, B. M. & Shears, N. T. Spatio-temporal patterns in coastal turbidity – Long-term trends and drivers of variation across an estuarine-open coast gradient. *Estuar. Coast. Shelf Sci.* **154**, 137–151 (2015).
81. Weis, J. et al. Southern ocean phytoplankton stimulated by wildfire emissions and sustained by iron recycling. *Geophys. Res. Lett.* https://doi.org/10.1029/2021gl097538 (2022).
82. Vergara, I., Garreaud, R. & Ayala, Á. Sharp increase of extreme turbidity events due to deglaciation in the subtropical Andes. *J. Geophys. Res. Earth Surf.* https://doi.org/10.1029/2021jf006584 (2022).
83. Schlegel, R. W. & Smit, A. J. heatwaveR: A central algorithm for the detection of heatwaves and cold-spells. *J. Open Source Softw.* **3**, 821 (2018).
84. WMO Guidelines on the Calculation of Climate Normals (WMO-No. 1203) (World Meteorological Organization Geneva, 2017).
85. Reed, D. & Miller, R. SBC LTER: hourly photon irradiance at the surface and seafloor, ongoing since 2008 ver 25. Environmental Data Initiative. *EDI Data Portal* https://doi.org/10.6073/pasta/9a42207dd4d2971cce4273fd8a1087b4 (2024).
86. Robinson, T. H., Leydecker, A., Keller, A. A. & Melack, J. M. Steps towards modeling nutrient export in coastal Californian streams with a Mediterranean climate. *Agric. Water Manag.* **77**, 144–158 (2005).
87. Page, H. M., Reed, D. C., Brzezinski, M. A., Melack, J. M. & Dugan, J. E. Assessing the importance of land and marine sources of organic matter to kelp forest food webs. *Mar. Ecol. Prog. Ser.* **360**, 47–62 (2008).
88. Aguilera, R. & Melack, J. M. Relationships among nutrient and sediment fluxes, hydrological variability, fire, and land cover in coastal California catchments. *J. Geophys. Res. Biogeosci.* **123**, 2568–2589 (2018).
89. Zeldis, J. R., Currie, K. I., Graham, S. L. & Gall, M. P. Attributing controlling factors of acidification and hypoxia in a deep, nutrient-enriched Estuarine Embayment. *Front. Mar. Sci.* https://doi.org/10.3389/fmars.2021.803439 (2022).
90. Morel, A. & Prieur, L. Analysis of variations in ocean color 1. *Limnol. Oceanogr.* **22**, 709–722 (1977).
91. Hicks, D. M. et al. Suspended sediment yields from New Zealand Rivers. *J. Hydrol.* **50**, 81–142 (2011).
92. Page, M., Reid, L. & Lynn, I. Sediment production from Cyclone Bola landslides, Waipaoa catchment. J. Hydrol. 38, 289–308 (1999).
93. Marden, M., Fuller, I. C., Herzig, A. & Betts, H. D. Badass gullies: fluvio-mass-movement gully complexes in New Zealand's East Coast region, and potential for remediation. *Geomorphology* **307**, 12–23 (2018).
94. Hicks, D. M., Gomez, B. & Trustrum, N. A. Event suspended sediment characteristics and the generation of hyperpycnal plumes at river mouths: East Coast Continental Margin, North Island, New Zealand. *J. Geol.* **112**, 471–485 (2004).
95. Lee, Z.-P. Diffuse attenuation coefficient of downwelling irradiance: an evaluation of remote sensing methods. *J. Geophys. Res.* https://doi.org/10.1029/2004jc002573 (2005).
96. Mitchell, J. et al. Undersea New Zealand, 1: 5,000,000. *NIWA Chart, Miscellaneous Series* **92** (2012).
97. Pinkerton, M. H., Gall, M., Steinmetz, T. & Wood, S. *NIWA Seas, Coasts and Estuaries New Zealand (NIWA-SCENZ): Image services of satellite (MODIS-Aqua) water quality products for coastal New Zealand. Data Product Version 1.0. Shiny-SCENZ Version 1.0*. https://gis.niwa.co.nz/portal/apps/experiencebuilder/template/?id=9794f29cd417493894df99d422c30ec2&page=page_8 (2022).

98. Hipel, K. W. & McLeod, A. I. *Time Series Modelling of Water Resources and Environmental Systems* (Elsevier, 1994).
99. Pohlert, T. trend: Non-Parametric Trend Tests and Change-Point Detection. R package version 1.1.6, https://CRAN.Rproject.org/package=trend (2023).

Acknowledgements

We gratefully acknowledge support from New Zealand MBIE Endeavour Fund Tau Ki Ākau UOWX2206, NIWA Marine Science SSIF, and the US National Science Foundation in support of the SBC LTER. We thank the NIWA-SCENZ project team: Simon Wood and Tilmann Steinmetz, as well as the NASA Ocean Biology Processing Group and MODIS project (USA), for remote sensing information and for making the NASA bio-Optical Marine Algorithm Dataset freely available on SeaBASS. We also thank all the people involved in acquiring and maintaining the long-term in situ light data in the Firth of Thames, New Zealand, and in the SBC LTER in California, USA. We thank Dr Antoine Minne for guidance on making the visual diagram shown as Fig. 7. Finally, we thank the three anonymous reviewers for their comments that helped improve the manuscript.

Author contributions

F.T. devised the project, the main conceptual ideas, and results, and wrote the initial manuscript. M.H.P., S.M., M.T. and D.R.S. contributed to the design and implementation of the research, to the analysis of the results and to the writing of the manuscript. D.R. and R.M. acquired, maintained and processed the SBC LTER light data. M.G. and J.Z. acquired, maintained and processed the New Zealand Firth of Thames coastal mooring light data. M.H.P., M.G. and F.T. contributed to the generation of the satellite remote sensing of seabed light. CB and DRS acquired most of the funding that supported the work in this manuscript. All co-authors (F.T., M.H.P., S.M., M.T., C.B., K.F.D., M.G., R.M., S.O., D.R., L.T., S.V., T.W., J.Z. and D.R.S.) contributed to the writing of the final manuscript.

Competing interests

The authors declare no competing interests

Additional information

Supplementary information The online version contains supplementary material available at https://doi.org/10.1038/s43247-025-03023-4.

Correspondence and requests for materials should be addressed to François Thoral.

Peer review information *Communications Earth and Environment* thanks Mark Baird, Craig G. Gelpi and the other anonymous reviewer(s) for their contribution to the peer review of this work. Primary Handling Editors: Olusegun Dada and Alice Drinkwater. A peer review file is available.